Double-differential inclusive hydrogen and helium spectra from neutron-induced reactions at 27.4, 39.7, and 60.7 MeV: Oxygen and nitrogen

T. S. Subramanian,* J. L. Romero, F. P. Brady, D. H. Fitzgerald,† R. Garrett,‡ G. A. Needham,§ J. L. Ullmann,** J. W. Watson,†† and C. I. Zanelli
Crocker Nuclear Laboratory and Department of Physics, University of California, Davis, California 95616

D. J. Brenner
Radiological Research Laboratory, College of Physicians and Surgeons of Columbia University, New York, New York 10032

R. E. Prael
Los Alamos National Laboratory, Los Alamos, New Mexico 87545
(Received 10 March 1986)

Double-differential cross sections for the neutron-induced production of p, d, t, ^{3}He, and alpha particles from oxygen and nitrogen have been measured using an unpolarized neutron facility. Neutron beam energies of 27.4, 39.7, and 60.7 MeV were used. The charged particle energy spectra, at six forward laboratory angles, 15, 20, 35, 40, 45, and 65, and, where feasible, at three backward angles, 90, 130, and 150 deg, range up to the kinematic maximum, from a typical low-energy cutoff of 4 MeV for p, d, t, and alpha particles, and 8 MeV for ^{3}He. Intranuclear cascade plus deexcitation calculations were carried out. The data are compared with these calculations and with available proton-induced (charge-symmetric) reaction spectra for oxygen.

I. INTRODUCTION

Despite their practical and theoretical importance, almost no inclusive measurements of secondary-charged particle spectra have been reported from neutron bombardment of oxygen and nitrogen. We present here the first measurements of double-differential cross sections for hydrogen and helium isotope production from oxygen and nitrogen at selected neutron energies in the 20–60 MeV range. Previously, a similar set of data was published for carbon in a paper[1] to be referred to as C.

The data presented are for incident neutron energies of 27.4, 39.7, and 60.7 MeV, which were chosen to facilitate comparison with the proton-induced cross section measurements performed at Oak Ridge.[2] The organization of this paper is similar to that of C.[1] The experimental setup is briefly discussed in Sec. II. Section III covers the data analysis and the normalization and corrections applied to the measured spectra and the errors assigned to them. An intranuclear cascade model followed by Fermi breakup, which is used to generate predictions of double-differential cross section spectra, is briefly described in Sec. IV. Discussion of the double-differential cross section data, along with comparisons with (i) the model predictions, and (ii) the charge symmetric proton-induced cross sections of Bertrand *et al.*[2] are presented in Sec. V.

II. EXPERIMENTAL DETAILS

The experimental setup was the same as described in C, and has been described in detail in Ref. 3. We review here its main features. Almost monochromatic neutron beams were produced from the ^{7}Li(p,n)^{7}Be ($Q = -1.64$ MeV) reaction.[4] The neutrons were collimated along 0 deg to strike a target located in an evacuated scattering chamber. The neutron spectrum consists of a peak that contains approximately 60% of the neutrons plus a rather flat low-energy tail.

Three-element, charged particle detector telescopes each consisting of a 50 μm Si (surface barrier) ΔE detector, a second 300–400 μm Si (surface barrier) ΔE detector, and a stopping E detector [NaI(Tl) or Si(Li)] were used for charged particle identification. Three such telescopes were positioned to cover, in all, nine laboratory angles, viz., 15, 20, 35, 40, 45, 65, 90, 130, and 150 deg. Combinations of ΔE vs E displays for energetic particles and particle velocity (time of flight) vs E displays for particles that stopped in the first detector element were used to identify charged particles spanning the entire energy range. In addition, a time-of-flight system with respect to a beam pickoff located upstream of the neutron-producing target was used to select only those events associated with the neutrons in the main peak.

Kodacel plastic ($C_3H_4O_2$) was used as a target for oxygen. The hydrogen in the compound facilitated simultaneous measurement of n-p cross sections for concurrent normalization. Two thin sheets of this material with a total thickness of 5.205 ± 0.068 mg/cm^2 were used as target.

For nitrogen, thin melamine targets ($C_3H_6N_6$) were prepared by evaporative coating of melamine on a Mylar base. Fairly rugged targets were obtained by alternating the side of the Mylar for each layer of coating. Target thicknesses were determined by weighing the target frames before and after evaporation. Several targets were also cut up for analysis. The results indicated that weighing the whole frame yielded thicknesses accurate to approximately 5%. Three different targets of evaluated thicknesses of 4.8 ± 0.2, 5.2 ± 0.15, and 5.0 ± 0.2 mg/cm^2

were used at neutron energies of 27.4, 39.7, and 60.7 MeV, respectively.

III. DATA REDUCTION

The procedure adopted in data reduction was as in C. Briefly, for each particle that provides an energy-loss signal in a detector, a timing pulse and an energy pulse height were obtained. For particles that passed through at least the first detector, a ΔE vs E scheme was used for particle identification. For those that stopped in the first detector, a time-of-flight vs E scheme was used. In all the cases, a neutron time-of-flight (TOF) cut was superimposed to select the events caused by the neutrons in the peak of the incident neutron beam. When a particle traversed more than one detector, the pulse heights from the active detectors were summed after matching their gains. Corrections for dead layers on detectors were also included. Two sets of energy channels (low and high gain) were provided for each of the ΔE detectors to facilitate better resolution between the helium and hydrogen particles. Since the helium particles at low energies lost a considerable portion of their energy in the target, these data were corrected for particle and energy loss in the target.[5] The alpha spectrum for $E < 8$ MeV contains some ^{3}He contamination produced by the neutron tail (see also Ref. 3). By comparing the measured ^{3}He and alpha cross sections in the region around 10 MeV, we estimate this contamination to be less than 5% at 60.7 MeV, less than 3% at 39.7 MeV, and negligible at 27.4 MeV.

The average low-energy thresholds for each detected particle were 3.8, 3.7, 4.1, 9.9, and 4.1 MeV for p, d, t, ^{3}He, and α, respectively, and generally correspond to those discussed in Table 1 of Ref. 3. For oxygen at 39.7 MeV, the deuteron threshold at angles other than 20° and 40° was 11.6 MeV. For protons, owing to the presence of hydrogen in the target, the effective thresholds at forward angles increased up to about 8 MeV, depending on the beam energy and scattering angle. This is due to the time-of-flight wraparound of elastic n-p products from the neutron beam tail. For the full energy neutrons, the elastic n-p reaction also introduces gaps in the proton spectra. These gaps shift in energy rapidly with angle.

Absolute cross sections were obtained by normalizing to the n-p elastic cross section using the parametrization of Binstock,[6] our previously measured n-p cross sections,[7] and a knowledge of the hydrogen content of the target used. The overall normalization uncertainty is estimated to be 5% for oxygen and 10% for nitrogen compounded with the uncertainty in the n-p cross section (typically 3—5%).[8] The average detector angular resolution was 3° and the neutron beam energy width was approximately 2 MeV. Correction for background and carbon content in the targets was done by subtracting with a CH target (as in C), both related by a suitable monitor.

Additional data obtained by Needham *et al.*[9] on protons and deuterons from nitrogen and oxygen at the neutron incident energy of approximately 60 MeV have been combined with the present data. That data were obtained with a higher threshold (~ 12 MeV) using a gas target and covers only forward angles ($\leq 65°$).

IV. THEORETICAL MODEL

The model used was as described in C. Briefly, the intranuclear cascade calculations were performed with a code based on the Monte Carlo method outlined by Chen *et al.*,[10] although without provision for pion production, implying an upper energy limit of around 300 MeV. This code allows for a description of the nucleus in terms of nucleons, alpha clusters, and two-nucleon clusters. We have taken spectroscopic factors—the measure of finding a cluster in the nucleus—from the work of Balashov *et al.*,[11] whose calculations in turn agree with the results of cluster "knockout" experiments on carbon and oxygen. Thus, the ^{16}O nucleus is taken to be a time average of 2.52 alpha clusters plus 5.92 nucleons, whilst the ^{14}N nucleus is taken to be represented by 1.64 alpha clusters plus 5.44 nucleons plus one two-nucleon cluster. The nucleus is assumed to be spherically symmetric and to consist of a series of 18 annular spherical shells, each with a density obtained from two-parameter Fermi distributions derived from electron elastic scattering.[12] In each shell Fermi-momentum distributions for nucleons are calculated, based on the nucleon density in that region. For the clusters, which are bosons, a Fermi momentum distribution appropriate to the density normalized to a single particle is used. For nucleon scattering, Pauli blocking is enforced, such that a collision is only allowed if both nucleons have a final energy greater than their Fermi energies. Particle emission is restricted by one and two particle separation energies, which are updated on a time-dependent basis to take into account prior particle emissions, and to ensure energy conservation. Finally, particles are allowed to escape freely when their radial position approximately exceeds the half-density radius of the nucleus.

We have also included a simple model for nucleon transfer, in particular, the nucleon pickup reaction yielding a deuteron, a process known to contribute significantly to the charged particle yield.[13] In the spirit of the intranuclear cascade we have followed the conceptual approach used in Ref. 13, whereby on-shell transfer cross sections were successfully used. As a first approach, these transfer cross sections are estimated using the plane-wave Born approximation as described by Selove.[14]

When no further direct emission is energetically possible, the type, energy, and direction of all emitted particles and the compound nucleus are recorded, and another incident particle treated. Typically 10^5 incident particles are used for the cascade program, taking, for nitrogen at 60 MeV, around 30 min on a CRAY X-MP computer.

The compound nuclei formed in the cascade must be allowed to deexcite. As discussed elsewhere (see, for example, Ref. 15), the use of an evaporation model to describe the particle emission from an equilibrium compound nucleus is not realistic for light nuclei. Therefore, we use an approach, termed "Fermi breakup," suggested initially by Bohr and by Fermi,[16] and subsequently used by, among others, Zhdanov and Fedotov[17] and Gradsztajn *et al.*[18] Fermi pointed out that if the energy of the collision is dumped into a small nuclear volume, it will be rapidly statistically redistributed among the degrees of freedom of

the system. This conclusion will be true independent of the number of particles in the volume. All possible final states will then appear with frequencies proportional to their statistical weights. Thus, the breakup probability for all possible channels may be computed, and a particular channel chosen by random-number techniques.

In contrast to earlier implementations of the Fermi breakup technique, we have recognized that a considerable number of decays go through particle-unstable intermediate states, and we have thus allowed multiple, sequential decays.

Some other novel features of the code are the use of a Coulomb barrier penetration factor, derived from Coulomb wave functions, for two-body breakup (the most common type); for multiparticle breakup, a simple threshold is used, adjusted for Coulomb energy. Again for the most commonly found two-body breakup, parity and isospin conservation are enforced, as well as a restriction of particle emission by a neutral-particle angular momentum barrier. For carbon and oxygen in the range below about 100 MeV, eight-body breakup is sufficiently unlikely to allow restriction of calculating probabilities only up to seven-body breakup. If much higher energies are required, the code could be extended, though with an increase in running time.

Finally, and very importantly, up to date experimental data are used as the data base for mass excesses, excitation energies, spins, isospins, and parities of all available nuclear levels.

Computing time for the breakup calculation was considerably less than for the cascade, and the use of 10^5 initial neutrons resulted in statistical uncertainties in double-differential spectra that were typically less than 10%.

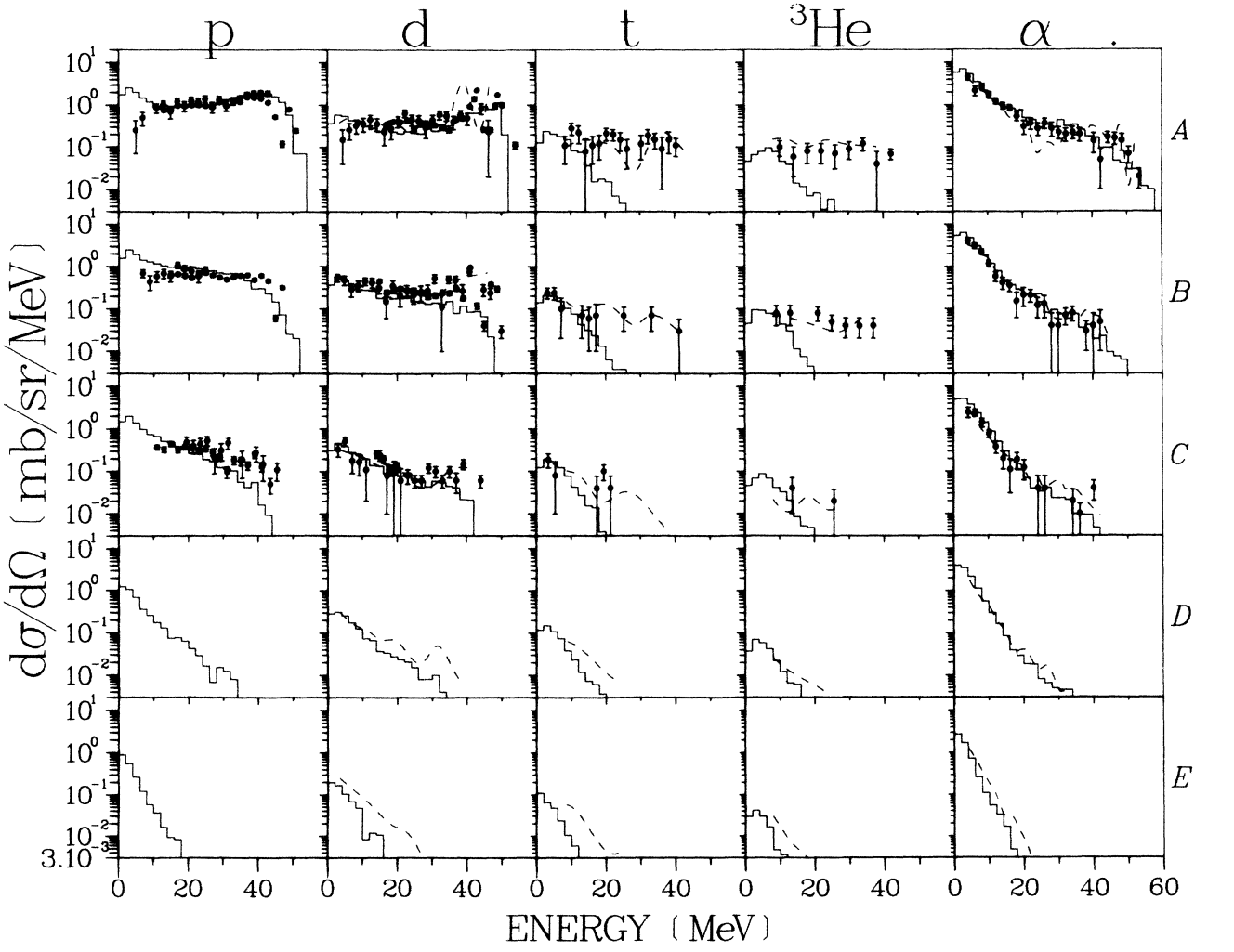

FIG. 1. Results from oxygen at 61 MeV. For key to plots see Table I. The results of the calculations are shown as histograms. The dashed curves are spline fits to the corresponding charge-symmetric proton-induced data from Ref. 2.

TABLE I. Key to Figs. 1–3 (for oxygen).

	Fig. 1			Fig. 2			Fig. 3		
	Neutron experiment	Neutron calculation	Proton experiment	Neutron experiment	Neutron calculation	Proton experiment	Neutron experiment	Neutron calculation	Proton experiment
Energy (MeV):	60.7	60.7	61.9	39.7	39.7	38.8	27.4[a]	27.4	28.8
Key									
A	20°	15°–25°	15°	20°	15°–25°	20°	15°	5°–15°	
B	40°	35°–45°	40°	40°	35°–45°	45°	35°	25°–35°	30°
C	65°	55°–65°	65°	60°[b,c]	55°–65°	60°	65°	55°–65°	
D		89°–95°	90°	90°[b,d]	85°–95°	90°	90°	85°–95°	
E		155°–165°	160°	130°	125°–135°		130°	125°–135°	

[a]Due to experimental constraints prevailing during the data collection run, no data could be extracted for ^{3}He at 27.4 MeV.
[b]No ^{3}He or tritons above our experimental threshold (8 MeV).
[c]α data from neutron experiment at 65°.
[d]p and α data at 80°, calculation at 75°–85°.

V. RESULTS AND DISCUSSION

Some representative results (experiment and calculation) for oxygen are shown in Figs. 1–3. (See also Table I.) Also shown are the results of the corresponding charge-symmetric measurements[2] for proton-induced reactions on oxygen, whereby (n,xd) and (n,$x\alpha$) reactions are compared with (p,xd) and (p,$x\alpha$), but (n,xt) and (n,x ^{3}He) are compared with (p,x ^{3}He) and (p,xt), respectively. As expected, the proton- and neutron-induced data are in good agreement, increasing our confidence in the present measurements.

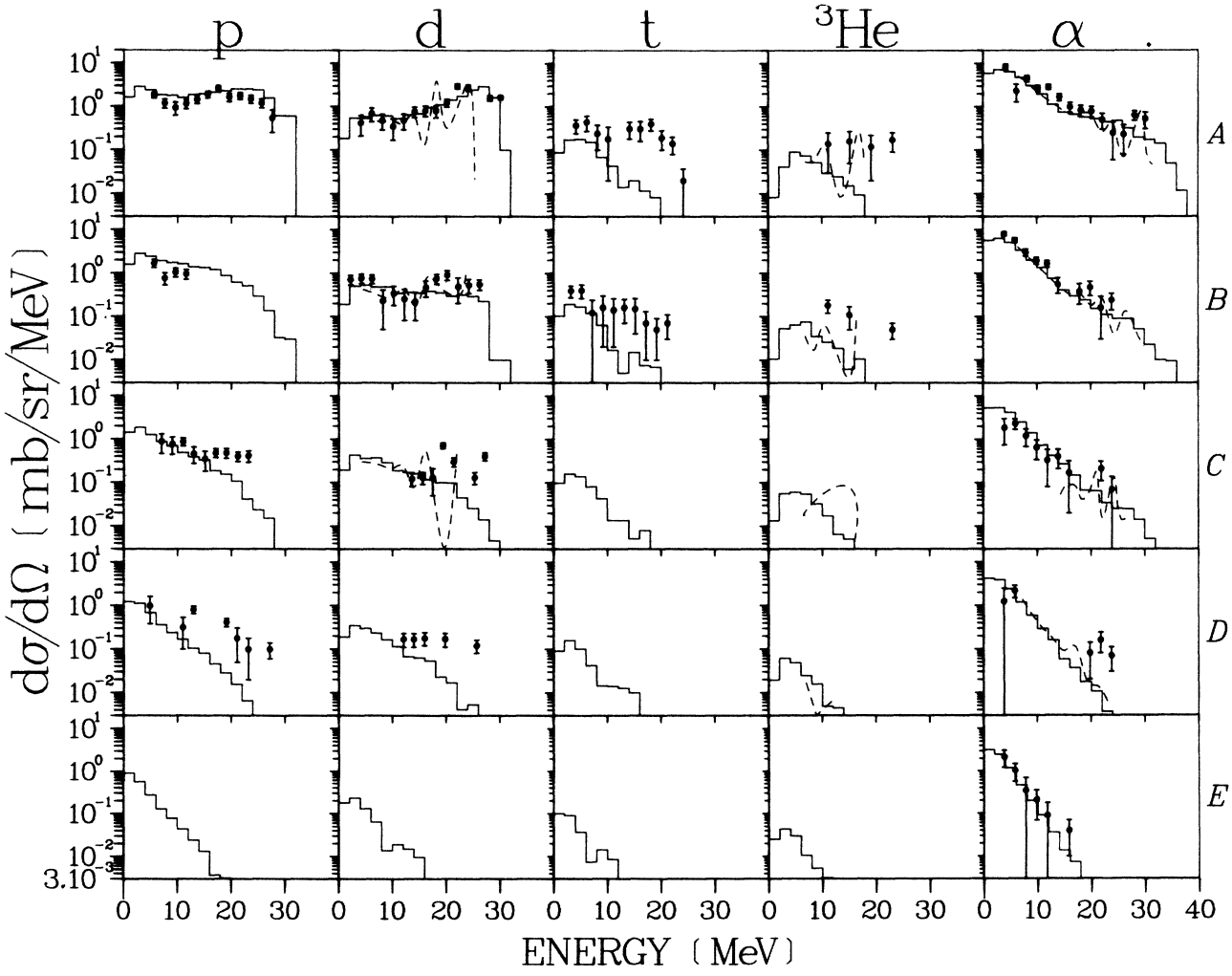

FIG. 2. Results at 40 MeV on oxygen. See caption to Fig. 1.

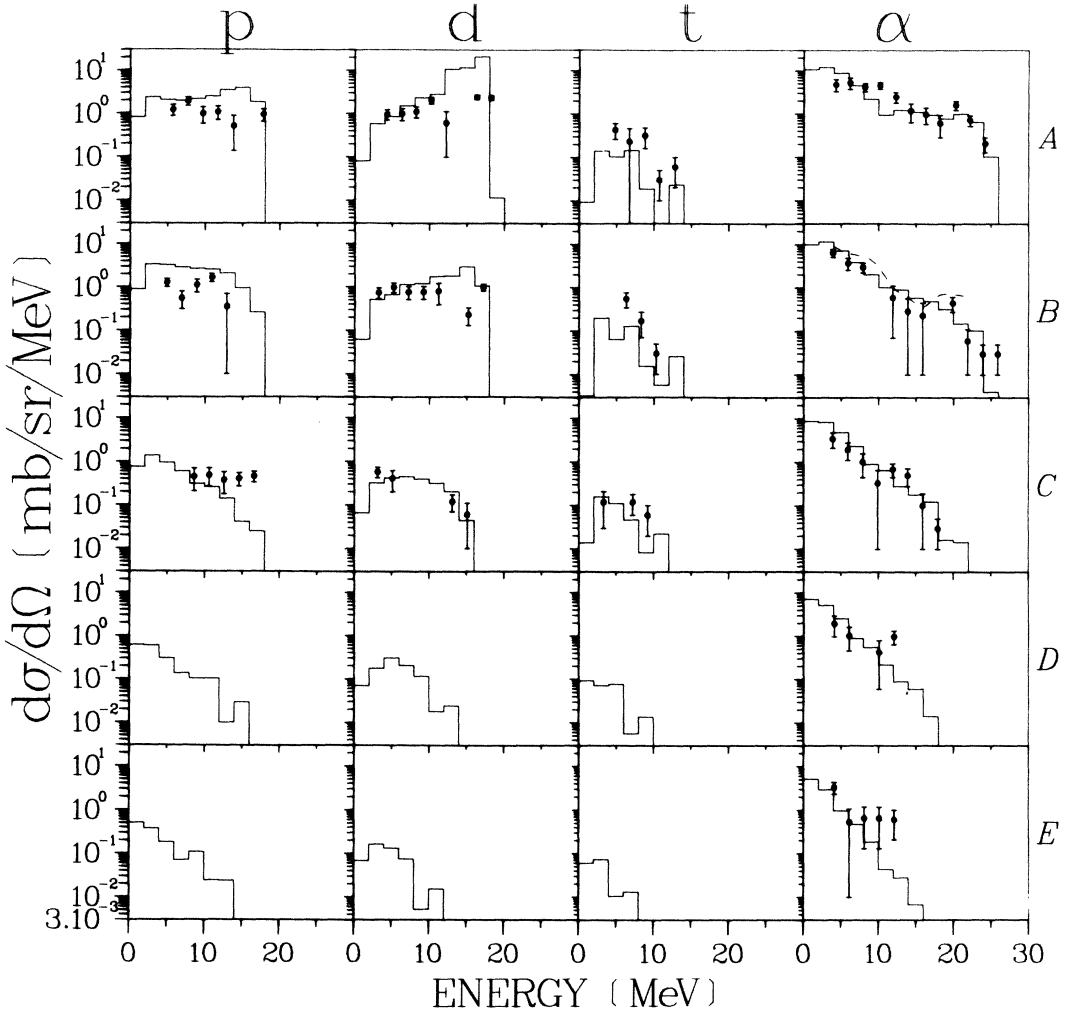

FIG. 3. Results at 27 MeV on oxygen. See caption to Fig. 1.

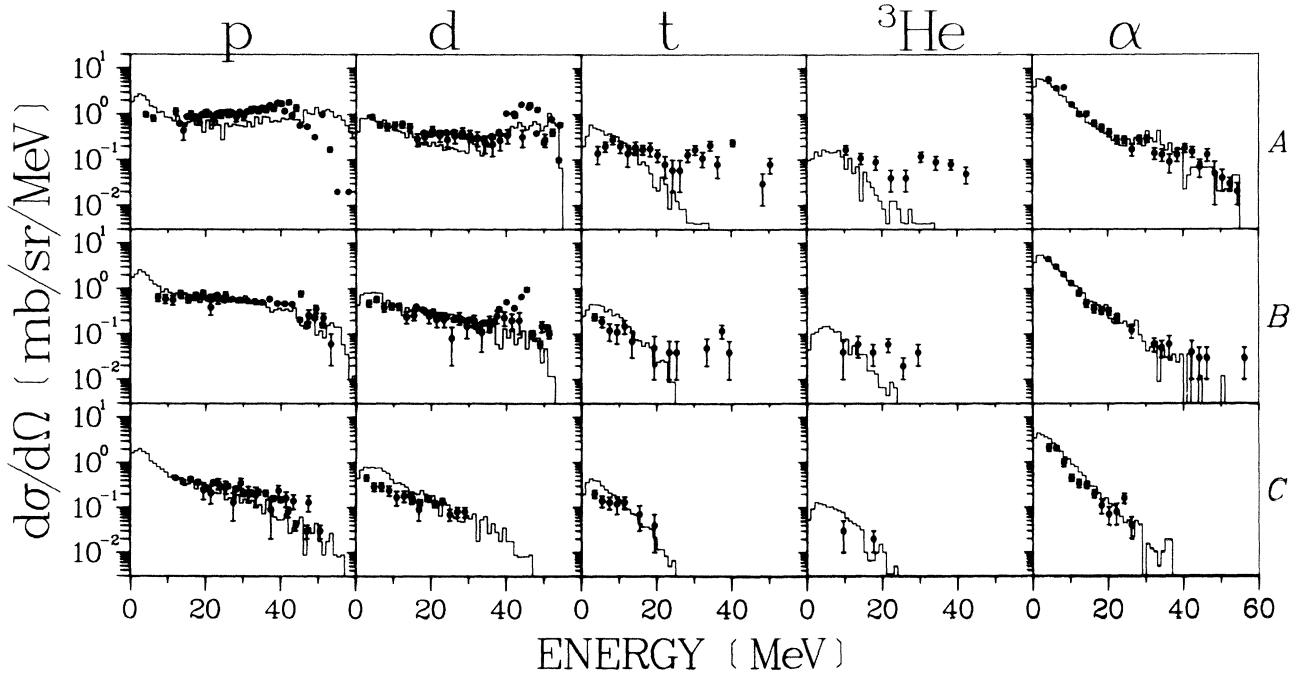

FIG. 4. Results from nitrogen at 61 MeV. For key to plots see Table II. The results of the calculations are shown as histograms.

TABLE II. Key to Figs. 4–6 (for nitrogen).

	Fig. 4		Fig. 5		Fig. 6	
	Neutron experiment	Neutron calculation	Neutron experiment	Neutron calculation	Neutron experiment	Neutron calculation
Energy (MeV):	60.7	60.7	39.7	39.7	27.4	27.4
Key						
A	20°	15°–25°	20°	15°–25°	20°	15°–25°
B	40°	35°–45°	40°	35°–45°	40°	35°–45°
C	65°	55°–65°	65°	55°–65°	65°	55°–65°
D			90°	85°–95°	90°	85°–95°
E			150°	145°–155°	130°	125°–135°

Comparisons between the measurements and calculations yield similar conclusions to those obtained for carbon in C. In general the agreement is surprisingly good, since the assumptions of cascade models are usually thought to be breaking down at energies much below 100 MeV.[19] It might be pointed out here that the model contains no "fitting" parameters. At forward angles the agreement is very good for secondary protons, deuterons, and alphas, although there is a suggestion of an overprediction of low-energy protons, due to the assumption (see Sec. IV) that particles escape freely when their radial position exceeds the half-density radius. The triton and ^{3}He spectra are less well predicted, presumably because transfer reactions yielding these particles were not modeled.

At backward angles, although the experimental data are

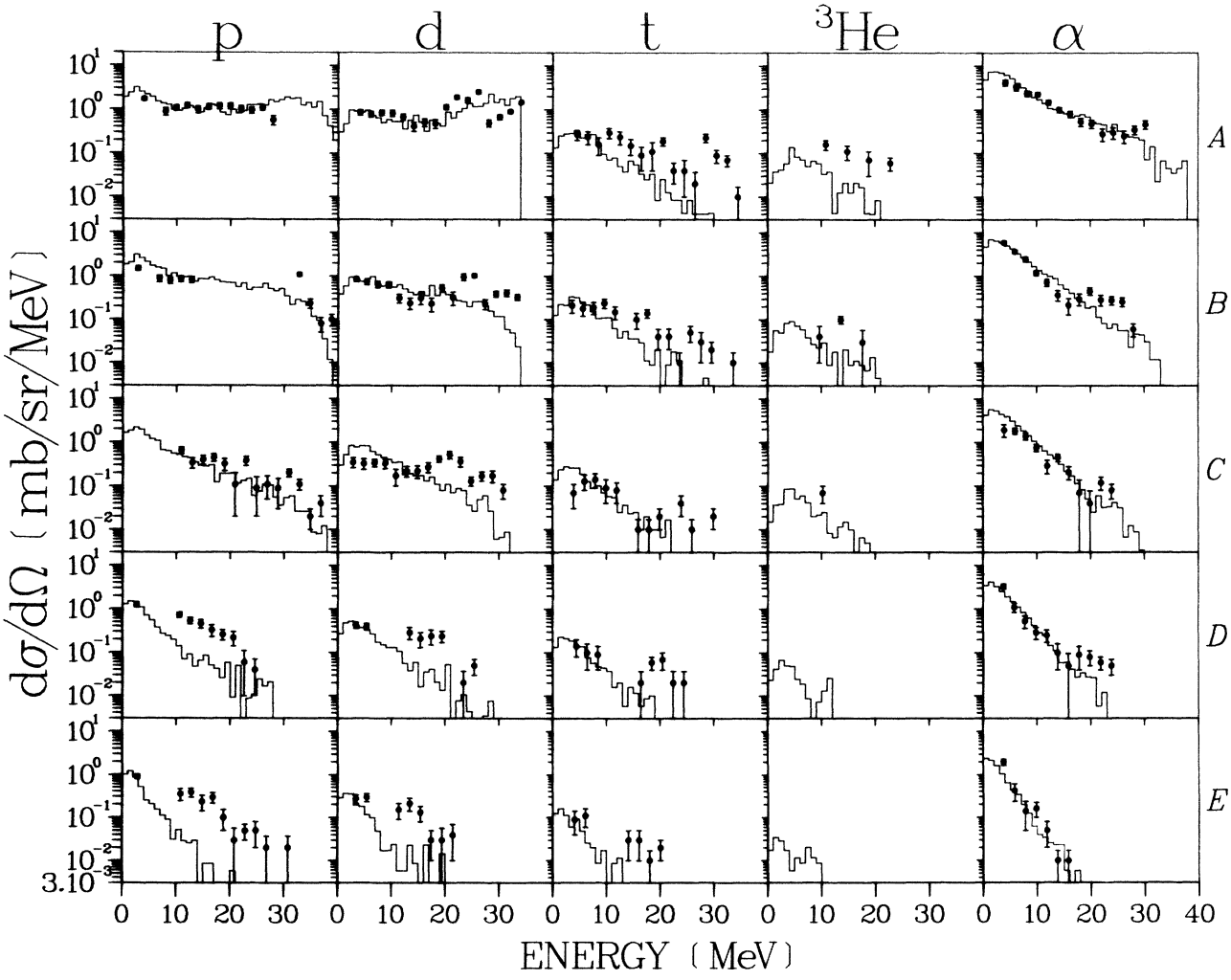

FIG. 5. Results at 40 MeV on nitrogen. See caption to Fig. 4.

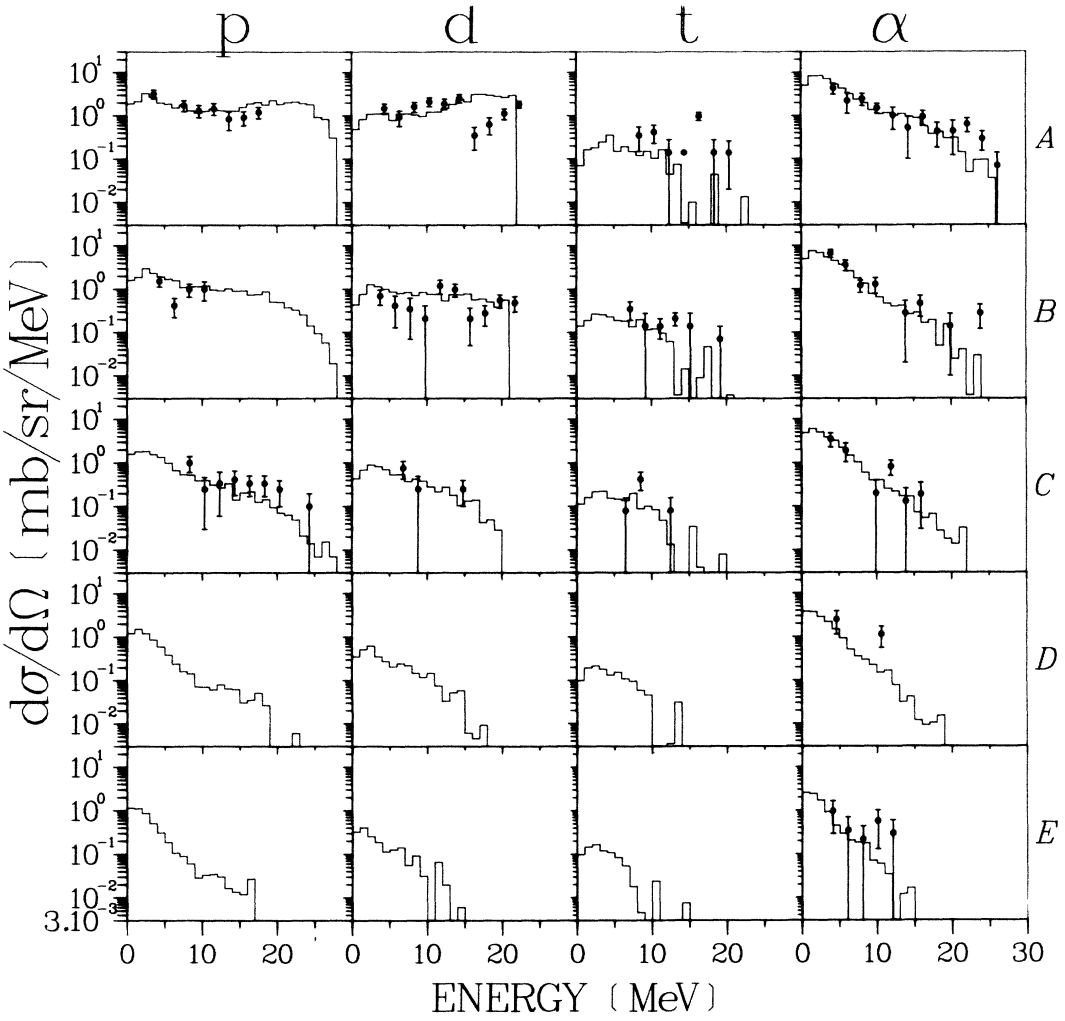

FIG. 6. Results at 27 MeV on nitrogen. See caption to Fig. 4.

more limited, it is clear that too few high-energy protons and deuterons are predicted. As discussed in the earlier paper C, it is hard to see how these high-energy large-angle particles could be produced in our model, which only utilizes two-body interactions.

The experimental data for nitrogen and the corresponding calculations are shown in Figs. 4—6. (See also Table II.) Essentially all the same trends are present as previously observed for carbon and oxygen. The increased kinematic limit for secondary protons is, of course, due to the decrease in separation energy.

VI. CONCLUSIONS

We have presented the first comprehensive set of inclusive hydrogen and helium double-differential spectra after neutron bombardment of oxygen and nitrogen. The data have been compared with the corresponding proton-induced results (oxygen only) yielding good agreement, and with intranuclear cascade/Fermi breakup calculations. Agreement with the calculations is surprisingly good, particularly at forward angles.

Only a representative selection of results have been shown here. Full details of the experimental results at all angles may be obtained from J.L.R. Microfiche containing detailed results of the calculations, including kerma factors, at incident neutron and proton energies between 10 and 150 MeV for carbon, nitrogen, and oxygen may be obtained from D.J.B.

ACKNOWLEDGMENTS

We would like to thank E. Russell, J. McCurdy, and the Crocker Nuclear Laboratory crew for providing a variety of beams in the preparatory and the executional phases of this experiment. We also thank Dr. Vic Viola and Dr. Ali Gokmen for providing us with the original version of the cascade code. We acknowledge the support of NCI (Grants CA-16261 and CA-15307), the NSF (Grants PHY71-03400 and PHY77-05301), and DOE (Contract DE-AC02-83ER-60142).

*Permanent address: Memorial Hospital Radiation Center, Hollywood, FL 33021.

†Present address: Department of Physics, University of California—Los Angeles, Los Angeles, CA 90024.

‡Permanent address: Department of Physics, University of Auckland, Auckland, New Zealand.

§Permanent address: Rocketdyne Division, Rockwell, Canoga Park, CA 91304.

**Present address: Nuclear Physics Laboratory, University of Colorado, Boulder, CO 80309.

††Permanent address: Department of Physics, Kent State University, Kent, OH 44242.

[1]T. S. Subramanian, J. L. Romero, F. P. Brady, J. W. Watson, D. H. Fitzgerald, R. Garrett, G. A. Needham, J. L. Ullmann, C. I. Zanelli, D. J. Brenner, and R. E. Prael, Phys. Rev. C **28**, 521 (1983), to be referred to as C.

[2]F. E. Bertrand and R. W. Peelle, Phys. Rev. C **8**, 1045 (1973); Oak Ridge National Laboratory Report ORNL-4799, 1973.

[3]T. S. Subramanian, J. L. Romero, and F. P. Brady, Nucl. Instrum. Methods **174**, 475 (1980).

[4]J. A. Jungerman and F. P. Brady, Nucl. Instrum. Methods **89**, 167 (1970).

[5]M. L. Johnson, J. L. Romero, T. S. Subramanian, and F. P. Brady, Nucl. Instrum. Methods **169**, 179 (1980).

[6]J. Binstock, Phys. Rev. C **10**, 19 (1974).

[7]T. C. Montgomery, F. P. Brady, B. E. Bonner, W. B. Broste, and M. W. McNaughton, Phys. Rev. Lett. **31**, 640 (1973); Phys. Rev. C **16**, 499 (1977); N. S. P. King, J. D. Reber, J. L. Romero, D. H. Fitzgerald, J. L. Ullmann, T. S. Subramanian, and F. P. Brady, Phys. Rev. C **21**, 1185 (1980).

[8]T. S. Subramanian, Ph.D. thesis, University of California, 1979, p. 91.

[9]G. A. Needham, F. P. Brady, D. H. Fitzgerald, J. L. Romero, J. L. Ullmann, J. W. Watson, C. Zanelli, N. S. P. King, and G. R. Satchler, Nucl. Phys. **A385**, 349 (1982).

[10]K. Chen, Z. Fraenkel, G. Friedlander, J. R. Groves, J. M. Miller, and Y. Shimamato, Phys. Rev. **166**, 949 (1968).

[11]V. V. Balashov, A. N. Boyarkina, and I. Rotter, Nucl. Phys. **59**, 417 (1964).

[12]C. W. DeJager, H. de Vries, and C. de Vries, At. Data Nucl. Data **14**, 479 (1976).

[13]F. Hachenberg, H. C. Chiang, and J. Hufner, Phys. Lett. **97B**, 183 (1980).

[14]W. Selove, Phys. Rev. **101**, 231 (1956).

[15]E. Gross, University of California Report UCRL-3330, 1956.

[16]E. Fermi, Prog. Theor. Phys. **5**, 570 (1950).

[17]A. P. Zhdanov and P. I. Fedotov, Zh. Eksp. Teor. Fiz. **45**, 455 (1963) [Sov. Phys. JETP **18**, 313 (1964)].

[18]M. Epherre and E. Gradystajn, J. Phys. (Paris) **28**, 747 (1967).

[19]D. J. Brenner, Phys. Med. Biol. **29**, 437 (1984).